Sensors and Materials, Vol. 37, No. 2 (2025) 553–556
MYU Tokyo

S & M 3932

Ba-fresnoite Single-crystalline Scintillator for X-ray Detection

Kensei Ichiba,[1*] Kenichi Watanabe,[2] Kai Okazaki,[1] Takumi Kato,[1]
Daisuke Nakauchi,[1] Noriaki Kawaguchi,[1] and Takayuki Yanagida[1]

[1]Nara Institute of Science and Technology, Takayama, Ikoma, Nara 630-0192, Japan
[2]Kyusyu University, 744 Motooka, Nishi-ku, Fukuoka 819-0395, Japan

(Received October 31, 2024; accepted December 13, 2024)

Keywords: scintillator, $Ba_2TiSi_2O_8$, single crystal, floating zone method

Scintillation detectors, composed of scintillators and photodetectors, have recently been applied in various fields. Since the performance of scintillation detectors mainly depends on that of the scintillator, the development of more advanced scintillators is still ongoing. In this study, Ba-fresnoite is focused on as a new scintillator and its performance is evaluated. Ba-fresnoite shows an emission band centered at 460 nm with decay time constants of 1.0 and 3.7 ms, and the light yield is 5100 photons/MeV.

1. Introduction

Scintillation detectors have recently been actively employed in various fields such as medical,[1] security,[2] and well logging.[3] Such detectors are composed of scintillators and photodetectors.[4] Scintillators are optical materials that convert the energy of ionizing radiation into low-energy photons, and photodetectors can change the low-energy photons from scintillators into electric signals. Since the performance of scintillation detectors strongly depends on that of scintillator, new scintillators with more advanced performance have been developed.[5–16]

Scintillation detectors are categorized into pulse-counting or current-type detectors depending on their application. For example, pulse-counting detectors are used in positron emission tomography to process individual radiation events, while current-type detectors are utilized for baggage inspection through signal integration over milliseconds. Hence, the required properties of scintillators vary slightly depending on whether pulse-counting or current-type detectors are used. In particular, scintillators in current-type detectors require high chemical stability, high emission intensity, high effective atomic number (Z_{eff}), high density, and low afterglow level.

The host material of interest in this study is Ba-fresnoite with the nominal composition $Ba_2TiSi_2O_8$. Ba-fresnoite has been investigated on regarding its ferroelectric,[17] piezoelectric,[18] and pyroelectric properties.[19] Additionally, Ba-fresnoite can be a promising scintillator because it has high chemical stability, relatively large Z_{eff} (48.1), and relatively high ρ (4.5 g/cm^3). In

*Corresponding author: e-mail: ichiba.kensei.if7@ms.naist.jp
https://doi.org/10.18494/SAM5426

ISSN 0914-4935
https://myukk.org/

previous studies, Ba-fresnoite showed a broad emission band in the range of 300–650 nm, which originated from the charge transfer (CT) from Ti^{4+} ions to O^{2-} ions.[19–21] The observed emission wavelength matches well with the wavelength sensitivity of some photodetectors such as photomultiplier tubes (PMTs). Nevertheless, Ba-fresnoite has never been studied as a scintillator. Therefore, we evaluated the scintillation properties of Ba-fresnoite to determine its potential for scintillator application.

2. Experimental Methods

A Ba-fresnoite single crystal was fabricated by the floating zone method. $BaCO_3$ (4N), TiO_2 (4N), and SiO_2 (4N) were mixed and sintered at 1200 °C for 10 h. The sintered mixture was formed into a cylinder rod that was resintered at 1200 °C for 8 h. After that, crystal growth was conducted, and the obtained crystalline rod was cut to obtain a measurement sample. To confirm the crystal phase, the powder X-ray diffraction (PXRD) pattern obtained with a MiniFlex600 diffractometer (Rigaku) was evaluated. The photoluminescence (PL) excitation/emission mapping, PL quantum efficiency (*QY*), and PL decay curve were evaluated with Quantaurus-QY (Hamamatsu, C11347-01) and Quantaurus-τ (Hamamatsu, C11367), respectively. The scintillation spectrum, decay curve, and pulse height spectrum (PHS) were evaluated with our original setups.[22–24]

3. Results and Discussion

Figure 1(a) shows a photograph and PXRD pattern of the fabricated sample. The sample size is approximately 4 × 4 × 1.0 mm^3, and the sample appears colorless and transparent. The PXRD pattern of the fabricated sample matches the reference from the International Centre for Diffraction Data (ICDD) No. 84–0924, and no additional peaks are detected. Thus, the fabricated sample has a single-phase structure of Ba-fresnoite. Figure 1(b) shows the PL excitation/emission mapping and decay curve of Ba-fresnoite. Under excitation at 260 nm, a broad emission band

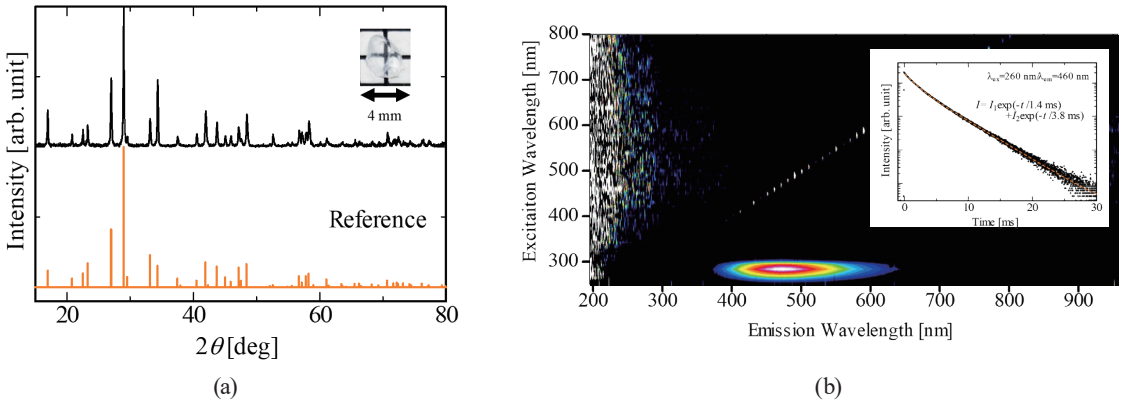

Fig. 1. (Color online) (a) Photograph and PXRD pattern of Ba-fresnoite. The reference pattern is ICDD No. 84–0924. (b) PL excitation/emission mapping and decay curve.

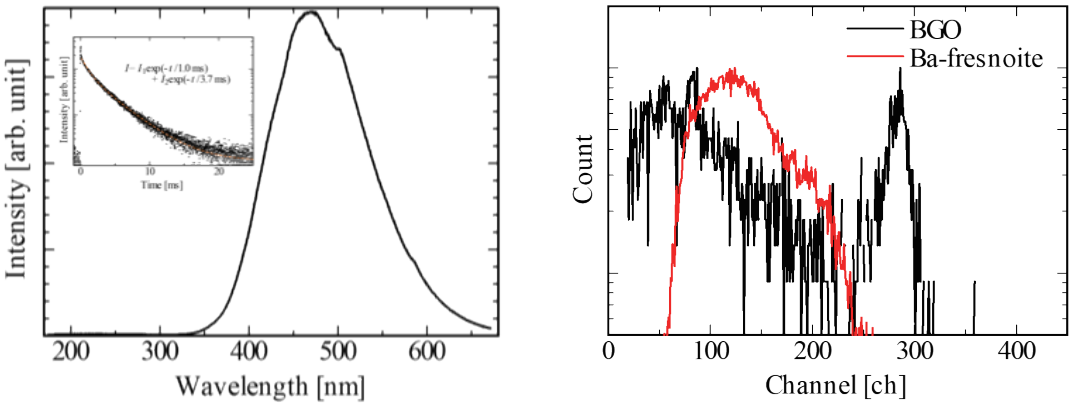

(a) (b)

Fig. 2. (Color online) (a) Scintillation spectrum, decay curve, and (b) PHS under γ-rays of Ba-fresnoite.

centered at 460 nm is observed and ascribed to the CT from Ti^{4+} ions to O^{2-} ions. Additionally, in a previous study, it was observed that the bandgap of $Ba_2TiSi_2O_8$ is ~4.7 eV.[19] Thus, the excitation band would originate from the transitions from the valence to the conduction band. The PL *QY* under excitation at 260 nm is 34.3% in the range of 300–700 nm. On the basis of the results of PL excitation/emission mapping, PL decay curve monitoring at 460 nm was evaluated under excitation at 260 nm. The PL decay curve is well fitted by the sum of two exponential functions, and the obtained decay time constants are 1.4 and 3.8 ms. Such constants would originate from the CT from Ti^{4+} ions to O^{2-} ions.[25,26]

Figure 2(a) shows the scintillation spectrum and decay curve of Ba-fresnoite. The scintillation spectrum of Ba-fresnoite shows a broad emission band in the range of 300–650 nm. To confirm the emission origin, the scintillation decay time profile was measured. The scintillation decay curve is well fitted by the sum of two exponential functions, and the observed decay time constants are 1.0 and 3.7 ms. Since the obtained values are comparable to the PL decay time constants, these constants originate from the CT from Ti^{4+} ions to O^{2-} ions. Thus, the emission band observed in the scintillation spectrum would also be ascribed to the CT from Ti^{4+} ions to O^{2-} ions. Comparison with other materials indicates the decay time constant of Ba-fresnoite is longer than that of commercial scintillators and is comparable to that of scintillators studied in the past for current-type detectors.[11,27–29] Figure 2(b) shows the PHS of Ba-fresnoite. $Bi_4Ge_3O_{12}$ (BGO) with a light yield (*LY*) of 8000 photons/MeV was used as a reference sample. Ba-fresnoite shows a photoabsorption peak at 194 ch. By comparing with the peak channel of BGO and the quantum efficiency of PMTs, the *LY* of Ba-fresnoite is calculated to be 5100 photons/MeV.

4. Conclusions

In this study, a Ba-fresnoite single crystal was synthesized and its performance as a scintillator was evaluated. The scintillation spectrum of Ba-fresnoite shows a broad emission band in the range of 300–650 nm, which originates from the CT from Ti^{4+} ions to O^{2-} ions. In

the pulse height spectra, the *LY* of Ba-fresnoite is estimated to be 5100 photons/MeV. Ba-fresnoite shows promise as a scintillator since the emission wavelength matches the wavelength sensitivity of PMTs. However, the *LY* is currently inferior to that of commercially available scintillators. In future work, the *LY* could be improved by incorporating rare-earth elements as dopant ions.

Acknowledgments

This work was supported by MEXT Grants-in-Aid for Scientific Research A (22H00309), Scientific Research B (23K21827, 23K25126, and 24K03197), Exploratory Research (22K18997), and JSPS Fellows (23KJ1591), and Asahi Glass Foundation and Suzuki Foundation.

References

1 P. Lecoq: Nucl. Instrum. Methods Phys. Res., Sect A **809** (2016) 130.
2 J. Glodo, Y. Wang, R. Shawgo, C. Brecher, R. H. Hawrami, J. Tower, and K. Shah: Phys. Procedia **90** (2017) 285.
3 C. L. Melcher: Nucl. Instrum. Methods Phys. Res., Sect B **40**–**41** (1989) 1214.
4 T. Yanagida: Proc. Jpn. Acad., Ser. B **94** (2018) 75.
5 Y. Endo, K. Ichiba, D. Nakauchi, T. Kato, N. Kawaguchi, and T. Yanagida: Sens. Mater. **36** (2024) 473.
6 N. Kawaguchi, T. Kato, D. Nakauchi, and T. Yanagida: Jpn. J. Appl. Phys. **62** (2023) 010611.
7 K. Okazaki, D. Nakauchi, A. Nishikawa, T. Kato, N. Kawaguchi, and T. Yanagida: Sens. Mater. **36** (2024) 587.
8 H. Fukushima, D. Nakauchi, T. Kato, N. Kawaguchi, and T. Yanagida: Jpn. J. Appl. Phys. **62** (2023) 010506.
9 D. Nakauchi, T. Kato, N. Kawaguchi, and T. Yanagida: Jpn. J. Appl. Phys. **62** (2023) 010607.
10 T. Yanagida, T. Kato, D. Nakauchi, and N. Kawaguchi: Sens. Mater. **34** (2022) 595.
11 T. Yanagida, T. Kato, D. Nakauchi, and N. Kawaguchi: Jpn. J. Appl. Phys. **62** (2023) 010508.
12 K. Ichiba, T. Kato, D. Nakauchi, N. Kawaguchi, and T. Yanagida: Sens. Mater. **36** (2024) 451.
13 H. Fukushima, D. Nakauchi, T. Kato, N. Kawaguchi, and T. Yanagida: Sens. Mater. **35** (2023) 429.
14 M. Koshimizu: Jpn. J. Appl. Phys. **62** (2023) 010503.
15 M. Koshimizu, Y. Fujimoto, and K. Asai: Sens. Mater. **35** (2023) 521.
16 Y. Takebuchi, A. Masuno, D. Shiratori, K. Ichiba, A. Nishikawa, T. Kato, D. Nakauchi, N. Kawaguchi, and T. Yanagida: Sens. Mater. **36** (2024) 579.
17 S. K. Barbar: New Materials, Processing and Manufacturability (Wiley, 2024) pp. 157–186.
18 C. Shen, H. Zhang, H. Cong, H. Yu, J. Wang, and S. Zhang: J. Appl. Phys. **116** (2014) 044016.
19 S. K. Barbar and M. Roy: J. Am. Ceram. Soc. **94** (2011) 843.
20 Y. Takahashi, T. Konishi, K. Soga, and T. Fujiwara: J. Ceram. Soc. Jpn. **116** (2008) 1104.
21 Z. Y. Mao and Y. C. Zhu: Mater. Res. Bull. **51** (2014) 197.
22 T. Yanagida, K. Kamada, Y. Fujimoto, H. Yagi, and T. Yanagitani: Opt. Mater. **35** (2013) 2480.
23 T. Yanagida, Y. Fujimoto, T. Ito, K. Uchiyama, and K. Mori: Appl. Phys. Express **7** (2014) 062401.
24 K. Watanabe, T. Yanagida, D. Nakauchi, and N. Kawaguchi: Jpn. J. Appl. Phys. **60** (2021) 106002.
25 G. Blasse: J. Inorg. Nucl. Chem. **41** (1979) 639.
26 Y. Takahashi, K. Kitamura, Y. Benino, T. Fujiwara, and T. Komatsu: Appl. Phys. Lett. **86** (2005) 091110.
27 Y. Endo, K. Ichiba, D. Nakauchi, H. Fukushima, K. Watanabe, T. Kato, N. Kawaguchi, and T. Yanagida: Solid State. Sci. **145** (2023) 107333.
28 D. Nakauchi, K. Watanabe, T. Kato, N. Kawaguchi, and T. Yanagida: Nucl. Instrum. Methods Phys. Res., B **546** (2024) 165167.
29 T. Kunikata, K. Watanabe, P. Kantuptim, D. Shiratori, T. Kato, D. Nakauchi, N. Kawaguchi, and T. Yanagida: Radiat. Phys. Chem. **216** (2024) 111454.